ACS Medicinal Chemistry Letters
Cite This: ACS Med. Chem. Lett. 2019, 10, 627−632
Letter
pubs.acs.org/acsmedchemlett

Identification of Isoform 2 Acid-Sensing Ion Channel Inhibitors as Tool Compounds for Target Validation Studies in CNS

Leda Ivanova Bencheva,[†] Marilenia De Matteo,[†] Luca Ferrante,[†] Marco Ferrara,[†,#] Adolfo Prandi,[†] Pietro Randazzo,[†] Silvano Ronzoni,[†] Roberta Sinisi,[†] Pierfausto Seneci,[†,∥] Vincenzo Summa,[§] Mariana Gallo,[§] Maria Veneziano,[§] Antonella Cellucci,[§] Nausicaa Mazzocchi,[‡] Andrea Menegon,[‡,⊥] and Romano Di Fabio*[,†,§,⊥]

[†]Promidis, Via Olgettina 60, 20132 Milan, Italy
[‡]San Raffaele Scientific Institute, Experimental Imaging Center, ALEMBIC, Advanced Light and Electron Microscopy BioImaging Center, Via Olgettina 60, 20132 Milan, Italy
[§]IRBM Science Park, Via Pontina Km 30.600, 00070 Pomezia, Rome, Italy
[∥]Chemistry Department, Università degli Studi di Milano, Via Golgi 19, I-20133 Milan, Italy

Supporting Information

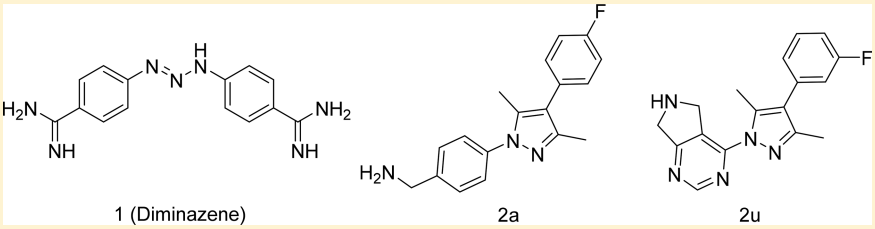

ABSTRACT: Acid-sensing ion channels (ASICs) are a family of ion channels permeable to cations and largely responsible for the onset of acid-evoked ion currents both in neurons and in different types of cancer cells, thus representing a potential target for drug discovery. Owing to the limited attention ASIC2 has received so far, an exploratory program was initiated to identify ASIC2 inhibitors using diminazene, a known *pan*-ASIC inhibitor, as a chemical starting point for structural elaboration. The performed exploration enabled the identification of a novel series of ASIC2 inhibitors. In particular, compound **2u** is a brain penetrant ASIC2 inhibitor endowed with an optimal pharmacokinetic profile. This compound may represent a useful tool to validate in animal models *in vivo* the role of ASIC2 in different neurodegenerative central nervous system pathologies.

KEYWORDS: *ASICs, ion channels, drug discovery, CNS, PNS, cancer*

The variation of proton concentration in tissues is a tightly controlled process.[1] In particular, a decrease of pH has been observed both in physiological conditions, i.e., control of neuronal functions by proton-mediated signaling, and pathological conditions.[2,3] Notably, acidification occurring in pathological conditions was found to recruit acid-sensing ion channels (ASICs), a family of proton-activated ion channels[4] that are highly expressed both in central and peripheral neurons[5] and in different types of cancer cells,[6] thus representing a potential target for drug discovery.[3,7] ASICs are voltage-insensitive ion channels belonging to the ENaC/DEG channel superfamily, which includes epithelial Na^+ channels (ENaC) and degenerins (DEG). Four ASICs genes (*ASIC1−4*) and two specific splice variants for ASIC1 and ASIC2 (a and b) have been described in mammals to date. ASIC1a, ASIC2a, and ASIC2b are primarily expressed in central nervous system (CNS) neurons, while all subunits are expressed in the peripheral nervous system (PNS). ASIC1a, ASIC2a, and ASIC3 subunits assemble to form both homotrimeric and heterotrimeric channels, whereas ASIC2b and ASIC4 only contribute to forming heteromeric channels with other ASIC subunits.[7,8] In terms of electrophysiology, while ASIC1a undergoes rapid inactivation, for ASIC2 and ASIC3 a noninactivated current potentially relevant in chronic pathologies, was observed. Thus far, both ASIC1 and ASIC3 have been extensively studied,[9] while ASIC2 has received much less attention. Notably, ASIC2 has recently been proposed as a relevant target in some forms of cancer,[10,11] whereas, in combination with ASIC1 subunits, it appears to play a key role in neuronal physiopathology.[12] Several natural peptides and synthetic small molecules, i.e., diminazene **1** (DA, Chart 1), an anti-infective veterinary drug, have been described as ASICs inhibitors.[13−15] However, the latter compound shows both poor target and ASIC isoform specificity, along with negligible blood−brain barrier (BBB) penetration, hence limiting its usage as therapeutic agent both for CNS and

Special Issue: Highlighting Medicinal Chemistry in Italy

Received: November 30, 2018
Accepted: February 7, 2019
Published: February 7, 2019

DOI: 10.1021/acsmedchemlett.8b00591
ACS Med. Chem. Lett. 2019, 10, 627−632

Chart 1. Structure of Diminazene (DA)1 and Early Lead2a

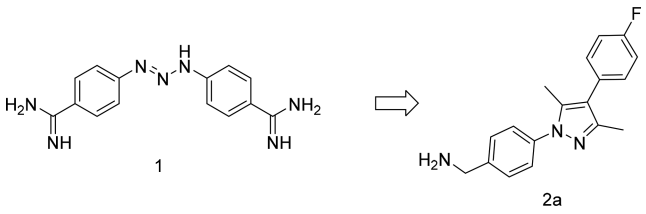

PNS pathologies.[16,17] Therefore, an exploratory project was initiated, using DA as chemical starting point, to obtain brain penetrant ASIC2 inhibitors as useful tool compounds for target validation studies in CNS. To this aim, ASIC1a and ASIC2a being the most highly expressed ASIC subunits in CNS neurons, the new chemical entities (NCEs) synthesized were specifically tested for their effects on murine homotrimeric ASIC1a and ASIC2a, and on heterotrimeric ASIC1a/2a.[18]

To identify the most appropriate methodology for *in vitro* screening of NCEs, a series of published data[19−21] on both compound **1** and amiloride, a diuretic drug known to interact with ASICs, specifically caught our attention. An optical technology based on membrane potential detection by voltage-sensitive dyes (VSDs)[22−25] was proposed. This original assay format showed an adequate throughput performance, and the ability to efficiently measure the inhibitory effect of ASICs-targeted NCEs. Moreover, additional evidence suggested the use of optic based assays, owing to the membrane potential sensitivity of ASIC1a binding affinity to small molecules.[20]

The preliminary structural elaboration of DA, in three sequential steps, enabled the identification of 1,4-diaryl, 3−5-dimethylpyrazole derivative **2a** (Chart 1), an early lead compound that was fully characterized in terms of ASICs inhibition. In particular, the linear triazene linker present in DA was initially replaced by a 1,3-disubstituted five-membered heterocycle, with the aim to rigidify the molecular core. Then, to reduce the basic character of the molecule, with the aim to improve its drug-like character and possibly secure BBB permeability, one of the two amidine functions was successfully removed. Finally, an initial exploration was made on the effect of the substitution of terminal phenyl rings.

As shown in Table 1, compound **2a** exhibited greater *in vitro* activity than compound **1** and comparable activity on ASIC2a and ASIC1a/2a (IC_{50} = 18.9 and 10.9 μM, respectively), while being inactive on ASIC1a. Based on these preliminary encouraging results, the rapid "4 points" analoging exploration strategy depicted in Chart 2 was envisioned. Namely, we focused on the sequential elaboration of the two aryl moieties

Table 1. Compounds 2a−i: ASICs Inhibition[a]

entry	ASIC1a[a]	ASIC2a[a]	ASIC1a/2a[a]
1 (DA)	56.9 ± 8.9	169.0 ± 18.1	45.2 ± 8.8
2a	>30	18.9 ± 6.9	10.9 ± 1.6
2b	>30	>30	>30
2c	>30	8.8 ± 2.0	>30
2d	>30	16.3 ± 4.6	>30
2e	>30[b]	>30	>30
2f	>30	>30	>30
2g	>30	4.3 ± 0.5	>30
2h	>30	>30	>30
2i	>30	>30	>30

[a]IC_{50} were determined as described in the Supporting Information; they are expressed in μM and are the average value of at least n = 3 independent experiments ± SEM.

Chart 2. Structural Optimization of Early Lead2a

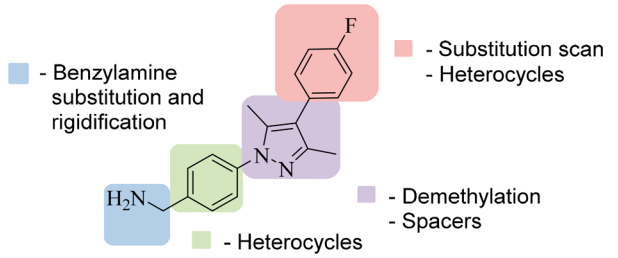

("pink and green"), the heterocycle core ("fuchsia"), and the suitable rigidification/masking of the potentially metabolically labile terminal benzyl function ("cyan").

At first, following the synthetic strategy shown in Scheme 1, nine "pink" analogues **2a−i** were synthesized. In particular, *p*-

Scheme 1. Variations on the 4-Aryl Substituent ("Pink"): Compounds 2a−i[a]

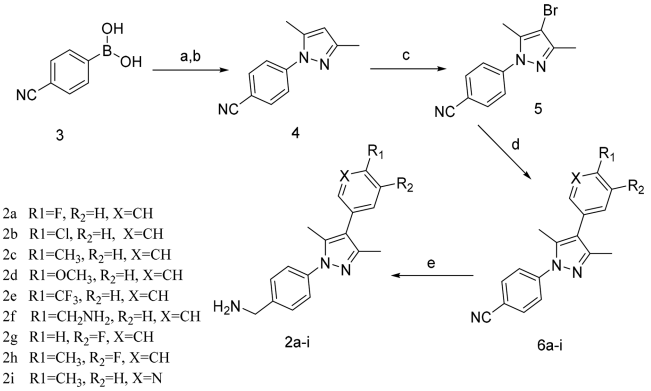

[a]Reagents and conditions: (a) di-*tert*-butyl diazene 1,2-dicarboxylate, $Cu(OAc)_2 \cdot H_2O$, MeOH, 65 °C, 1 h; (b) pentane-2,4-dione, 4 N HCl in dioxane, r.t., 10 min then 80 °C, 10 min, 76% (two steps); (c) NBS, EtOAc, sonication, 25−30 °C, 15 min, 80%; (d) substituted aryl/pyridinyl boronic acid, $Pd(PPh_3)_4$, aq. Na_2CO_3, DMF, microwave reactor, 140 °C, 15−20 min, 52%−70%; (e) $LiAlH_4$, THF, r.t, 0.5−3 h, 18−75%.

cyanophenyl boronic acid **3** was reacted with di-*tert*-butyl diazene 1,2-dicarboxylate and 2,4-pentanedione, to obtain 3,5-dimethyl pyrazole **4**. The following bromination reaction with NBS led to 4-bromo analogue **5**, which was coupled with nine different aryl or heteroaryl substituted boronic acids. The resulting 1-(*p*-cyanophenyl) pyrazoles **6a−i** were reduced to the corresponding benzylamines **2a−i** with lithium aluminum hydride in moderate to good overall yields.

The inhibition of ASICs constructs by compounds **2a−i** is reported in Table 1.

Monosubstituted compounds **2c** and **2d**, bearing a *p*-CH_3 or *p*-OCH_3 respectively, mostly retained the activity of the pyrazole early lead compound **2a**, while isoform selectivity for ASIC2a vs ASIC1a/2a was improved. Compound **2g**, the *m*-F analogue of **2a**, was the most potent and selective compound of this series. Notably, larger and/or charged functions (**2e**, p-CF_3; **2f**, p-CH_2NH_2), disubstituted aryls (**2h**, *p*-CH_3, *m*-F) and the presence of a pyridine as phenyl replacement (**2i**, *p*-CH_3, X = N) led to inactive compounds.

DOI: 10.1021/acsmedchemlett.8b00591
ACS Med. Chem. Lett. 2019, 10, 627−632

Then, the influence of the 3,5-dimethyl substituents present on the pyrazole core was evaluated by synthesizing the corresponding "fuchsia" des-methyl analogue **2j** (Scheme 2).

Scheme 2. Scaffold Hopping ("Fuchsia"): Des-methyl Compound 2j[a]

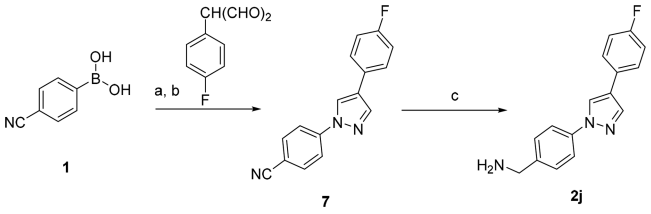

[a]Reagents and conditions: (a) di-*tert*-butyl diazene-1,2-dicarboxylate, $Cu(OAc)_2 \cdot H_2O$, MeOH, 65 °C, 1h; (b) 2-(4-fluorophenyl)-propanedial, 4 N HCl in dioxane, r.t., 10 min then 80 °C, 10 min, 56% two steps; (c) $LiAlH_4$, THF, r.t, 1h, 73%.

To this aim, *p*-cyanophenyl boronic acid **3** was treated with di-*tert*-butyl diazene-1,2-dicarboxylate in the presence of $Cu(OAc)_2 \cdot H_2O$ in MeOH at 65 °C for 1 h, followed by cooling to room temperature and addition of 2-(4-fluorophenyl)propanedial in 4 N HCl in dioxane initially at room temperature for 10 min, then at 80 °C for additional 10 min to give intermediate **7** in 56% yield. Then, reduction of the cyano group led to the corresponding benzylamine **2j** with lithium aluminum hydride in 73% yield.

Compound **2j** was inactive in terms of ASICs inhibition (IC_{50} > 30 μM on all ASICs constructs, Table 2), pointing out the relevance of both methyl groups for the recognition of the receptor binding site.

Table 2. Compounds 2k–w and 6a: ASIC Inhibition[a]

entry	ASIC1a[a]	ASIC2a[a]	ASIC1a/2a[a]
2a	>30	18.9 ± 6.9	10.9 ± 1.6
2j	>30	>30	>30
2k	>30	16.8 ± 5.4	>30
2l	>30	15.6 ± 2.9	>30
2m	>30	8.7 ± 2.3	>30
2n	>30	11.7 ± 2.7	>30
2o	>30	8.2 ± 1.5	>30
2p	>30	>30	>30
2q	>30	9.9 ± 1.1	11.3 ± 1.0
2r	>30	>30	>30
2s	>30	6.1 ± 1.1	8.5 ± 1.8
2t	>30	>30	>30
2u	>30	17.0 ± 4.7	>30
2v	>30	>30	>30
2w	>30	>30	>30
6a	>30	>30	>30

[a]IC_{50} were determined as described in the Supporting Information; they are expressed in μM and are the average value of at least n = 3 independent experiments ± SEM.

To acquire additional SAR information, a methylene spacer was introduced between N_1 of the pyrazole moiety ("fuchsia" compound **2k**, Scheme 3) by bromination and Suzuki coupling on 3,5-dimethyl pyrazole **8**, followed by alkylation at the N_1 position of 3,5-dimethyl pyrazole derivative **10a** with *p*-CN benzyl bromide, and by final reduction of the nitrile group with lithium aluminum hydride in poor, unoptimized yields.

Scheme 3. Spacer Introduction ("Fuchsia"): Compound 2k[a]

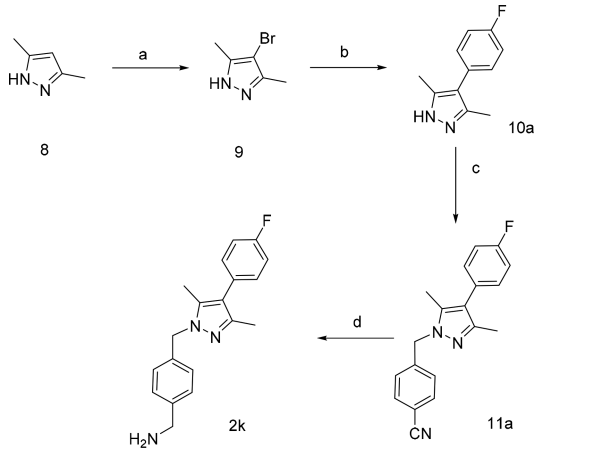

[a]Reagents and conditions: (a) NBS, EtOAc, sonication, 25–30 °C, 15 min, quantitative; (b) 4-(fluorophenyl)boronic acid or 3-(fluorophenyl)boronic acid, $Pd(PPh_3)_4$, sat. Na_2CO_3, DMF, 140 °C, 20 min, 70%; (c) 4-(bromomethyl)benzonitrile, Cs_2CO_3, CH_3CN, 50 °C, 10 h, quantitative; (d) $LiAlH_4$, THF, r.t, 1 h, 9%.

When compound **2k** was tested for its ability to inhibit ASICs, a comparable activity and isoform selectivity was observed for ASIC2a with respect to early lead **2a** (Table 2, IC_{50} = 16.8 and 18.9 μM, respectively).

Our attention was then focused on the "cyan" exploration by moving the *p*-benzylamine moiety from *para* to *meta* position of the phenyl ring (compound **2l**, Scheme 4), by introducing a methyl group at the benzylic position (compound **2m**, Scheme 4), or by C-1 homologation (compound **2n**, Scheme 4).

In particular, as for the synthesis of **2l**, 4-(*p*-fluorophenyl)-3,5-dimethyl pyrazole **10a** was *N*-arylated with *m*-cyanophenyl boronic acid using copper(II) acetate; the resulting 1-(*m*-cyanophenyl) pyrazole **12** was reduced to the corresponding benzylamine **2l** with lithium aluminum hydride in unoptimized poor yields. Compound **2m** was synthesized by reacting previously described 1-(*p*-cyanophenyl) pyrazole **6a** with methylmagnesium bromide in reducing conditions. Finally, compound **2n** was prepared from 4-(*p*-fluorophenyl)-3,5-dimethyl pyrazole **10a**, which was *N*-arylated with *p*-cyanomethyl phenyl bromide according to a Buchwald–Hartwig reaction experimental protocol[26] (microwave reaction, aqueous K_2CO_3 and DMSO, CuI, and L-proline, 140 °C, 26 h). The resulting pyrazole intermediate **13** was then reduced with sodium borohydride in the presence of cobalt(II) chloride to obtain the corresponding target benzylamine **2n**.

Compounds **2l**, **2m**, and **2n** mostly maintained the activity of the early pyrazole lead **2a** and showed high ASIC2a isoform-selectivity (Table 2), whereas the nitrile intermediate **6a** was inactive, pointing out the relevance of a primary amine function for ASICs inhibition.

The "cyan" exploration was expanded by constraining the amine function within a 5-membered ring. To this aim, compounds **2o–r** bearing a more symmetrical (**2o**, **2q**) or unsymmetrical amine (**2p**, **2r**), and a p-F (**2o**, **2p**) or m-F substituent at the 4-phenyl ring (**2q**, **2r**), were prepared. Their synthesis is reported in Scheme 5. Namely, previously described 4-(*p*-fluorophenyl)-3,5-dimethyl pyrazole intermediate **10a**, and 4-(*m*-fluorophenyl)-3,5-dimethyl pyrazole intermediate **10b** (prepared as **10a** in Scheme 3, using *m*-fluorophenyl boronic acid) were N-arylated with N-Boc-5-

DOI: 10.1021/acsmedchemlett.8b00591
ACS Med. Chem. Lett. 2019, 10, 627–632

Scheme 4. Variations on the Benzylamine ("Cyan"): Compounds 2l−n[a]

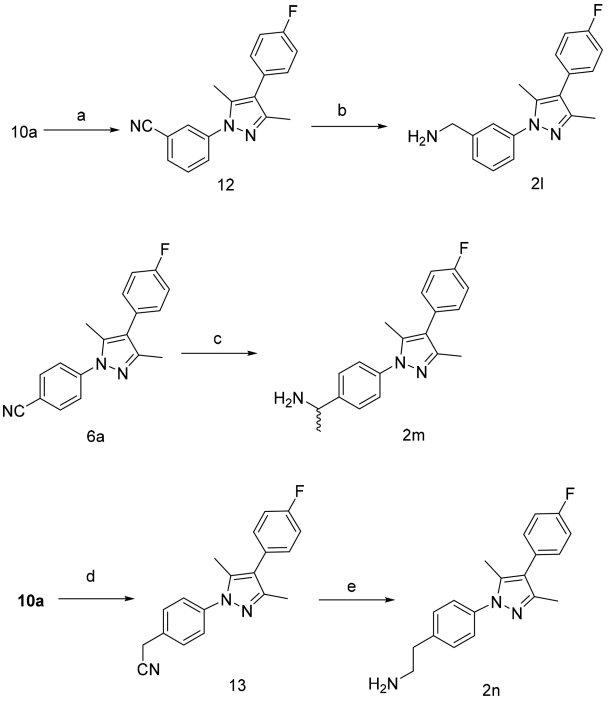

[a]Reagents and conditions: (a) 3-cyanophenylboronic acid, $Cu(OAc)_2·H_2O$, pyridine, DMF, 125 °C, 3 h, 11%; (b) $LiAlH_4$, THF, r.t, 3 h, 31%; (c) MeMgBr, THF, r.t, 5 h, then $LiAlH_4$, THF, 0° to r.t, 13%; (d) 4-bromobenzyl cyanide, CuI, L-proline, K_2CO_3, DMSO, 140 °C, 26 h, 33%; (e) $NaBH_4$, $CoCl_2$, MeOH, r.t, 1 h, 25%.

Scheme 5. Rigidification of the Benzylamine ("Cyan"): Compounds 2o−r[a]

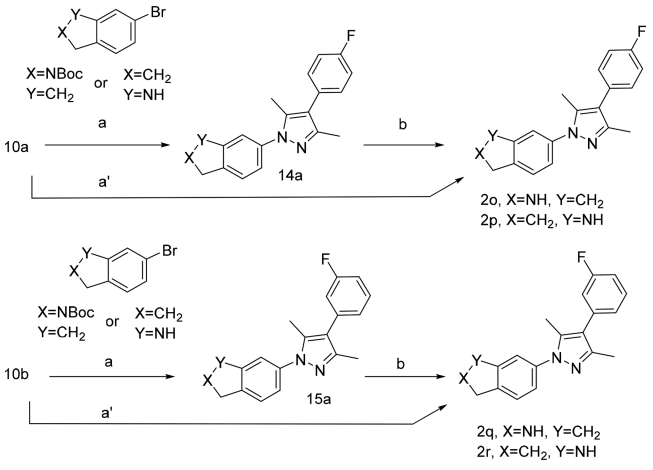

[a]Reagents and conditions: (a) *N*-Boc-5-bromo isoindoline, CuI, aqueous K_2CO_3, L-proline, DMSO, microwave, 75 °C, 4 h then 140 °C, 13 h, 42% (**14a**) or 15% (**15a**); (b) 4 N HCl in dioxane, 30 min, r.t., 32% (**2o**) or 63% (**2q**); (a′) 6-bromo indoline, aqueous K_2CO_3, CuI, L-proline, DMSO, microwave, 140 °C, 6 h, 44% (**2p**) or 13% (**2r**).

bromo isoindoline, using CuI in basic conditions in a microwave reactor.

The resulting *N*-Boc-protected 4-(*p*-fluorophenyl) pyrazoles **14a** and **15a** were obtained in 42% and 15% unoptimized yields, respectively. Then, removal of the *N*-Boc protecting group in acidic conditions afforded the corresponding target compounds **2o** and **2q** in 32% and 63% yields, respectively. Intermediates **10a** and **10b** underwent the same coupling reaction with 6-bromo indoline, obtaining the corresponding target compounds **2p** and **2r** in 44% and 13% yields, respectively (Scheme 5).

The inhibition of ASICs constructs by "cyan" compounds **2o−r** is reported in Table 2. In particular, the isoindoline derivative **2o** exhibited good *in vitro* activity and complete ASIC2a isoform selectivity. Conversely, compound **2q** inhibited both ASIC2a and ASIC1a/2a isoforms (IC_{50} = 9.9 and 11.3 μM, respectively). Notably, the corresponding indoline derivatives **2p** and **2r** were inactive.

Finally, the phenyl ring bearing the benzyl amine function was replaced ("green" exploration) by a 2-pyridine (**2s**) and a 3-pyridine (**2t**) ring, whereas dihydropyrrolo[3,4-*d*]pyrimidine homologues **2u** and **2v** and the *N*-Me derivative of the latter compound **2w** were prepared. Their synthesis is depicted in Scheme 6.

Previously described 4-(*p*-fluorophenyl)-3,5-dimethyl pyrazole intermediate **10a** was smoothly *N*-arylated with *p*-cyano-2-pyridyl fluoride in basic conditions (NaH in DMF); the resulting 1-(*p*-cyano-2-pyridyl) pyrazole **16** was reduced to the corresponding benzylamine derivative **2s** with lithium aluminum hydride in unoptimized, poor yields. Instead, the corresponding *m*-F analogue **2t** was synthesized from **10a** and 5-bromo-2-cyanopyridine using Cs_2CO_3, CuI, and 1,2-cyclohexanediamine. This coupling reaction was run in a microwave reactor for 13 h at 120 °C, and afforded cyano intermediate **17**, which was then reduced to amine **2t** in a poor, unoptimized 16% yield. Alternatively, compound **10a** was *N*-arylated with *tert*-butyl 4-chloro-5,7-dihydro-6*H*-pyrrolo[3,4-*d*]pyrimidine-6-carboxylate as seen earlier; the resulting *N*-Boc-protected pyrazole **18** was deprotected in acid conditions to yield the target compound **2u** in poor, unoptimized yields. Then, intermediate **10b** was transformed into the target compound **2v** by *N*-arylation followed by removal of the Cl atom by hydrogenolysis to give intermediate **20**, which was deprotected in acid conditions to the corresponding NH-free pyrazole **2v**. Finally, this compound was *N*-methylated to yield compound **2w** in good yields (Scheme 6).

As shown in Table 2, none of the compounds **2s−w** inhibited ASIC1a. The presence of a 2-pyridyl ring was well tolerated by ASIC2a (**2s**). Conversely, the presence of a 3-pyridyl ring led to complete inactivity (**2t**). The dihydropyrrolo[3,4-*d*]pyrimidine derivative **2u** was an ASIC2 inhibitor (IC_{50} = 17.0 μM) selective against the ASIC1a/2a heterodimer. Surprisingly, its close congeners **2v** and **2w**, bearing a 4-(*m*-fluorophenyl) substitution, resulted to be completely inactive.

Compound **2a**, **2o**, and **2u** were further profiled in terms of early physicochemical and ADME properties. *In vivo* PK characterization of **2u** over **2o** in mice was given priority, owing to its more drug-like physicochemical features (cLogP = 2.6 and 4.1; TPSA = 56 and 29 Å^2 for **2u** and **2o**, respectively). The summary of both the *in vitro* and *in vivo* characterization studies performed on **2a**, **2o**, and **2u** is reported in Table 3.

As for physicochemical descriptors, compound **2u** was significantly less lipophilic than **2a** and exhibited a greater TPSA value. Both compounds showed acceptable kinetic solubility and plasma protein binding (PPB). No inhibition of hERG was observed up to 30 μM concentration. In terms of inhibition of CYP450 isoforms, compound **2a** was found to

DOI: 10.1021/acsmedchemlett.8b00591
ACS Med. Chem. Lett. 2019, 10, 627−632

Scheme 6. Phenyl Substitution ("Green"): Compounds 2s–w[a]

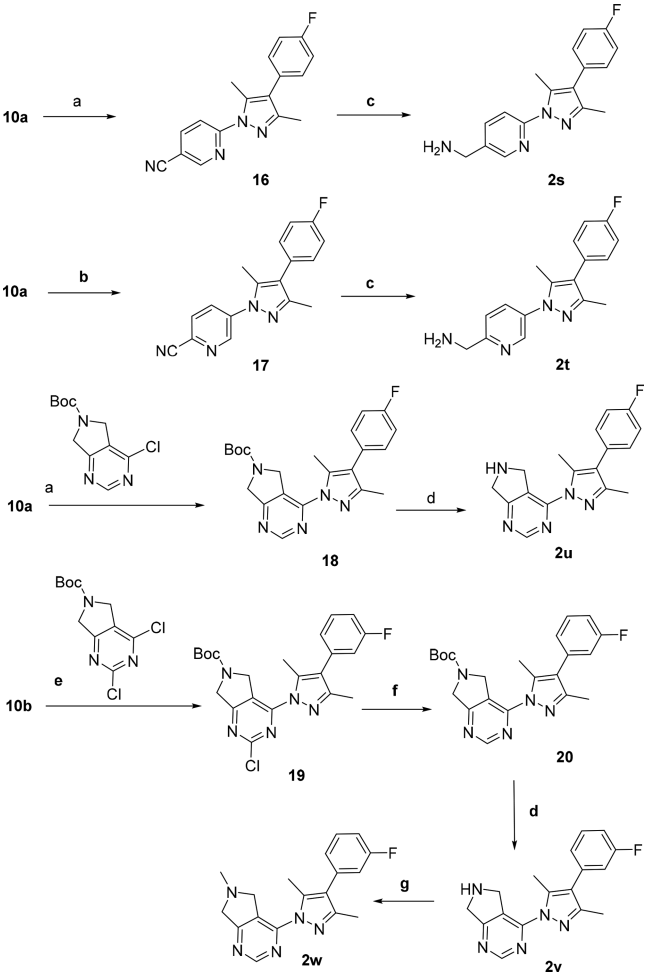

[a]Reagents and conditions: (a) 60% NaH, DMF, 0 °C, 30 min then 6-fluoronicotinonitrile, r.t, 1 h (98%, **16**) or *tert*-butyl 4-chloro-5,7-dihydro-6*H*-pyrrolo[3,4-*d*]pyrimidine-6-carboxylate, r.t., 1 h (9%, **18**); (b) 5-bromo-2-cyanopyridine, Cs_2CO_3, CuI, 1,2-cyclohexanediamine, microwave, 120 °C, 13 h, 19%; (c) $LiAlH_4$, THF, r.t, 1 h, 4% (**2s**), 16% (**2t**); (d) 4 N HCl in dioxane, r.t, 1–3 h, 8% (**2u**), 19% (**2v**); (e) 2/1 THF/DMF, DIPEA, microwave, 150°, 14 h, 58%; (f) H_2, TEA, MeOH, 10% Pd/C, 45 °C, 1 h; (g) formaldehyde, $NaCNBH_3$, MeOH, r.t, 1 h, 57%.

inhibit two different isoforms, i.e., 1A2 and 2D6, although at different extents, whereas **2u** inhibited only the 1A2 isoform. Particularly relevant were the differences observed in the *in vivo* pharmacokinetics in mice. Both compounds were tested at 1 mg/kg, i.v. and at 3 mg/kg, p.o. Notably, **2a** was highly cleared following i.v. administration (Cl = 224 mL/min/kg) but widely distributed in tissues (Vd = 50.9 l/kg), resulting in a low C_{max} after oral administration (C_{max} = 0.09 μM). However, being highly brain penetrant (B/P = 61), a relevant total brain concentration was observed after the administration of 1 mg/kg dose, i.v. (C_{max} = 2.46 μM). Conversely, compound **2u** showed a more balanced pharmacokinetic profile, owing to a sizable enhancement of the metabolic stability (Cl = 34 mL/min/kg) with respect to compound **2a**, an appropriate tissue distribution (Vd = 1.4 l/kg), complete absorption after oral administration (F = 100%) along with a significantly higher exposure p.o. with respect to **2a** ($C_{max=}$ 2.6 μM), and good

Table 3. ADME Profiling: Compounds 2a, 2o, and 2u

compound/assay	2a	2u	2o
cLogP[a]	3.9	2.6	4.2
TPSA (Å^2)[a]	44	56	30
solubility (μg/mL)[b]	73	32	56
PPB (%)[c]	93	94	95
h-ERG (IC_{50}, μM)	>30	>30	>30
CYP450 (IC_{50}, μM)[d]	0.4 [1A2]	0.8 [1A2]	0.2 [1A2] 4.8 [2D6]
Cl (mL/min/kg)[e]	224	34	NT
Vd (l/kg)	50.9	1.4	NT
C_{max} (μM)	0.09	2.6	NT
F (%)	60	100	NT
B/P ratio[f]	61	1.3	NT

[a]Calculated logP and topological polar surface area. [b]Kinetic solubility at pH 7.4. [c]% of bound compound to human serum albumin measured by NMR-based analysis. [d]Only CYP450 isoforms showing IC_{50} < 10 μM are reported; [e]*In vivo* PK studies were performed at 1 mg/kg, i.v. and at 3 mg/kg, p.o.; [f]Brain penetration studies were performed at 1 mg/kg, i.v. and B/P was calculated from 2 to 8 h after dosing.

brain penetration (B/P = 1.3). The relevant improvement of pharmacokinetic profile of **2u** vs **2a** was most likely due to the lack of the basic, metabolically labile primary benzylamine function present in compound **2a**, which was appropriately masked in **2u** within the constrained dihydropyrrolo[3,4-*d*]pyrimidine bicyclic moiety.

In conclusion, the described exploratory strategy enabled the identification of novel ASIC2 inhibitors. In particular, the "cyan" optimization approach focused on the stabilization of the terminal benzylamine function, which allowed to obtain compounds **2o** and **2u**, the selective ASIC2a-targeted *in vivo*-compliant lead compound. This compound, owing to its relevant drug-like character and balanced pharmacokinetic profile (including brain penetration), may represent a valuable tool compound to validate p.o. the role of ASIC2 *in vivo* in animal models of different type of CNS pathologies. In addition, **2u** can be seen as a foundation molecule for future optimization studies.

■ ASSOCIATED CONTENT

Supporting Information

The Supporting Information is available free of charge on the ACS Publications website at DOI: 10.1021/acsmedchemlett.8b00591.

Experimental procedures for the synthesis and the analytical characterization of both key intermediates and final compounds **2a–w** and **6a**, the *in vitro* screening of compounds **2a-w** and **6a**, and *in vivo* PK studies of compounds **2a** and **2u** (PDF)

■ AUTHOR INFORMATION

Corresponding Author

*Phone: +390249491701. E-mail: r.difabio@irbm.it.

ORCID

Romano Di Fabio: 0000-0003-1202-1354

Present Address

[#](M.F.) Flamma Innovation Srl, Via Cascina Secchi 217, 24040 Isso (BG), Italy.

DOI: 10.1021/acsmedchemlett.8b00591
ACS Med. Chem. Lett. 2019, 10, 627–632

Author Contributions

[⊥]These two authors share senior authorship.

Author Contributions

The manuscript was written through contributions of all authors. All authors have given approval to the final version of the manuscript.

Funding

The project was in part funded by the COLLEZIONE DEI COMPOSTI CHIMICI E CENTRO DI SCREENING−CNCCS scarl.

Notes

The authors declare no competing financial interest.

■ ACKNOWLEDGMENTS

The authors would like to thank Prof. Stefano Maiorana (Promidis), Dr. Edith Monteagudo (IRBM Science Park), Dr. Daniel Cicero (IRBM Science Park), and Dr. Annalise Di Marco (IRBM Science Park) for the useful discussion on the synthesis of the described chemical series, the *in vitro* and *in vivo* ADME studies, the serum albumin NMR-based analysis, and the CYP450 inhibition studies, respectively. In addition, thanks are due to Dr. Maria Rosaria Battista (IRBM Science Park) for the *in vitro* CYP450 inhibition studies.

■ ABBREVIATIONS

ASICs, acid-sensitive ion channels; DA, diminazene; ENaC, epithelial Na^+ channels; DEG, degenerins; CNS, central nervous system; PNS, peripheral nervous system; NCE, new chemical entity; VSD, voltage-sensitive dyes; BBB, blood−brain barrier; TPSA, topological polar surface area; PK, pharmacokinetic

■ REFERENCES

(1) Chesler, M. Regulation and modulation of pH in the brain. *Physiol. Rev.* **2003**, *83*, 1183−1221.
(2) Wemmie, J. A.; Taugher, R. J.; Kreple, C. J. Acid-sensing ion channels in pain and disease. *Nat. Rev. Neurosci.* **2013**, *14*, 461−471.
(3) Qadri, Y. J.; Rooj, A. K.; Fuller, C. M. ENaCs and ASICs as therapeutic targets. *Am. J. Physiol. Cell. Physiol.* **2012**, *302*, C943−965.
(4) Kellenberger, S.; Schild, L. International Union of Basic and Clinical Pharmacology. XCI. structure, function, and pharmacology of acid-sensing ion channels and the epithelial Na^+ channel. *Pharmacol. Rev.* **2015**, *67*, 1−35.
(5) Boscardin, E.; Alijevic, O.; Hummler, E.; Frateschi, S.; Kellenberger, S. The function and regulation of acid-sensing ion channels (ASICs) and the epithelial Na^+ channel (ENaC): IUPHAR Review 19. *Br. J. Pharmacol.* **2016**, *173*, 2671−2701.
(6) Liu, C.; Zhu, L. L.; Xu, S. G.; Ji, H. L.; Li, X. M. ENaC/DEG in Tumor Development and Progression. *J. Cancer* **2016**, *7*, 1888−1891.
(7) Wemmie, J. E.; Taugher, R. J.; Creple, C. J. Acid-sensitive ion channels in pain and disease. *Nat. Rev. Neurosci.* **2013**, *14*, 461−471.
(8) Kweon, H.-J.; Su, B.-C. Acid-sensing ion channels (ASICs): therapeutic targets for neurological diseases and their regulation. *BMB Rep.* **2013**, *46*, 295−304.
(9) Li, W. G.; Xu, T. L. ASIC3 channels in multimodal sensory perception. *ACS Chem. Neurosci.* **2011**, *2*, 26−37.
(10) Zhou, Z. H.; Song, J. W.; Li, W.; Liu, X.; Cao, L.; Wan, L. M.; Tan, Y. X.; Ji, S. P.; Liang, Y. M.; Gong, F. The acid-sensing ion channel, ASIC2, promotes invasion and metastasis of colorectal cancer under acidosis by activating the calcineurin/NFAT1 axis. *J. Exp. Clin. Cancer Res.* **2017**, *36*, 130.
(11) Vila-Carriles, W. H.; Kovacs, G. G.; Jovov, B.; Zhou, Z. H.; Pahwa, A. K.; Colby, G.; Esimai, O.; Gillespie, G. Y.; Mapstone, T. B.; Markert, J. M.; Fuller, C. M.; Bubien, J. K.; Benos, D. J. Surface expression of ASIC2 inhibits the amiloride-sensitive current and migration of glioma cells. *J. Biol. Chem.* **2006**, *281*, 19220−19232.
(12) Wu, J.; Xu, Y.; Jiang, Y. Q.; Xu, J.; Hu, Y.; Zha, X. M. ASIC subunit ratio and differential surface trafficking in the brain. *Mol. Brain* **2016**, *9*, 4.
(13) Baron, A.; Lingueglia, E. Pharmacology of acid-sensing ion channels - Physiological and therapeutical perspectives. *Neuropharmacology* **2015**, *94*, 19−35.
(14) Chen, X.; Qiu, L.; Li, M.; Dürrnagel, S.; Orser, B. A.; Xiong, Z.-G.; MacDonald, J. F. Diarylamidines: high potency inhibitors of acid-sensing ion channels. *Neuropharmacology* **2010**, *58*, 1045−53.
(15) Lingueglia, E.; Lazdunski, M. Pharmacology of ASIC channels. *Wiley Interdiscip. Rev. Membr. Transp. Signal.* **2013**, *2*, 155−171.
(16) Chen, X.; Orser, B. A.; MacDonald, J. F. Design and screening of ASIC inhibitors based on aromatic diamidines for combating neurological disorders. *Eur. J. Pharmacol.* **2010**, *648*, 15−23.
(17) Zhou, J.; Le, V.; Kalia, D.; Nakayama, S.; Mikek, C.; Lewis, E. A.; Sintim, H. O. Diminazene or berenil, a classic duplex minor groove binder, binds to G-quadruplexes with low nanomolar dissociation constants and the amidine groups are also critical for G-quadruplex binding. *Mol. BioSyst.* **2014**, *10*, 2724−2734.
(18) Liu, Y.; Hagan, R.; Schoellerman, J. Dual action of Psalmotoxin at ASIC1a and ASIC2a heteromeric channels (ASIC1a/2a). *Sci. Rep.* **2018**, *7179*, 1−11.
(19) Dorofeeva, N. A.; Barygin, O. I.; Staruschenko, A.; Bolshakov, K. V.; Magazanik, L. G. Mechanisms of non-steroid anti-inflammatory drugs action on ASICs expressed in hippocampal interneurons. *J. Neurochem.* **2008**, *106*, 429−441.
(20) Schmidt, A.; Rossetti, G.; Joussen, S.; Gründer, S. Diminazene Is a Slow Pore Blocker of Acid-Sensing Ion Channel 1a (ASIC1a). *Mol. Pharmacol.* **2017**, *92*, 665−675.
(21) Krauson, A. J.; Rooney, J. G.; Carattino, M. D. Molecular basis of inhibition of acid sensing ion channel 1A by diminazene. *PLoS One* **2018**, *13* (5), No. e0196894.
(22) Huang, C.-J.; Harootunian, A.; Maher, M. P.; Quan, C.; Raj, C. D.; McCormack, K.; Numann, R.; Negulescu, P. A.; González, J. E. Characterization of voltage-gated sodium-channel blockers by electrical stimulation and fluorescence detection of membrane potential. *Nat. Biotechnol.* **2006**, *24*, 439−446.
(23) Mazzocchi, N.; De Ceglia, R.; Mazza, D.; Forti, L.; Muzio, L.; Menegon, A. Fluorescence-Based Automated Screening Assay for the Study of the pH-Sensitive Channel ASIC1a. *J. Biomol. Screening* **2016**, *21*, 372−380.
(24) Menegon, A.; Pitassi, S.; Mazzocchi, N.; Redaelli, L.; Rizzetto, R.; Rolland, J. F.; Poli, C.; Imberti, M.; Lanati, A.; Grohovaz, F. A new electro-optical approach for conductance measurement: an assay for the study of drugs acting on ligand-gated ion channels. *Sci. Rep.* **2017**, *7*, 44843.
(25) For further details, see the method for optical measuring variations of cell membrane conductance reported in patents EP2457088, WO 2011009825 and US 13/386225.
(26) Heravi, M. M.; Kheilkordi, Z.; Zadsirjan, K.; Heydari, M.; Malmir, M. Buchwald-Hartwig reaction: an overview. *J. Organomet. Chem.* **2018**, *861*, 17−104.

DOI: 10.1021/acsmedchemlett.8b00591
ACS Med. Chem. Lett. 2019, 10, 627−632